Dentomaxillofacial Radiology (2008) 37, 268–273

http://dmfr.birjournals.org

RESEARCH

Dosimetry of the cone beam computed tomography Veraviewepocs 3D compared with the 3D Accuitomo in different fields of view

E Hirsch[1], U Wolf[2], F Heinicke[2] and MAG Silva*[,1,3]

[1]*Department of Dentomaxillofacial Radiology, Dental School, University of Leipzig, Germany;* [2]*Centre for Radiotherapy and Radio Oncology, University of Leipzig, Germany;* [3]*Department of Stomatologic Sciences, Federal University of Goias School of Dentistry, Goias, Brazil*

Objectives: This study compares tissue-absorbed and effective doses of the cone beam CT (CBCT) units, the Veraviewepocs 3D and the 3D Accuitomo, in different protocols.
Methods: The absorbed organ doses were measured using an anthropomorphic phantom loaded with thermoluminescent dosemeters (TLDs) in 16 sensitive organ sites. Both CBCT units were deployed with different fields of view (FOVs): 3D Accuitomo using two protocols (anterior 4×4 cm scan and anterior 6×6 cm scan) and Veraviewepocs 3D using three protocols (anterior 4×4 cm scan, anterior 8×4 cm scan and panoramic + anterior 4×4 cm). Equivalent and effective doses were then calculated, the latter based on the International Commission on Radiological Protection's (ICRP) 2005 recommendations.
Results: The lowest effective dose was observed for the 3D Accuitomo 4×4 cm (20.02 μSv), the highest for the 3D Accuitomo 6×6 cm (43.27 μSv). The effective dose recorded for Veraviewepocs 3D was 39.92 μSv for the 8×4 cm scan, 30.92 μSv for the 4×4 cm scan and 29.78 μSv for the panoramic + 4×4 cm scan protocol.
Conclusions: The radiation doses delivered by both machines were in comparable ranges when using 4×4 cm FOV. A smaller FOV should be used for dental images, whereas a larger FOV should be restricted to cases in which a wider view is required.
Dentomaxillofacial Radiology (2008) **37,** 268–273. doi: 10.1259/dmfr/23424132

Keywords: thermoluminescent dosimetry; tomography, X-ray computed; radiography, panoramic; cone beam computed tomography

Introduction

Successful dental treatment is always based on thorough planning and this usually necessitates the use of images. The need to assess the spatial relationships of anatomical structures and measurements and the evaluation of tissue density have all increased the prescription of three-dimensional (3D) and cross-sectional images in recent times. Consequently, both conventional imaging and CT have been widely used in dentistry and, in many instances, CT examinations are the first or even the main diagnostic imaging procedure undertaken. However, CT scanners are large and expensive systems primarily designed for full-body scanning. The cone beam CT (CBCT) scanner is intrinsically three-dimensional (3D) in its acquisition of images, and provides usable images from systems that are so compact and inexpensive that they can be installed in minor diagnostic centres.[1,2] CBCT provides high resolution imaging, diagnostic reliability and risk-benefit assessment. Hence, it is believed that this cutting-edge technology supplies the ideal examination for such dentomaxillofacial practices as dental implants,[3,4] oral surgery,[5,6] endodontic practice,[7,8] periodontal measurements,[9] temporomandibular joint examinations[10,11] and orthodontic procedures.[12–15] In addition, the radiation dose received by the patient is markedly lower than doses from conventional[16] or multislice CT.[17,18] CBCT results in doses that are three to seven times those of panoramic doses and 40% less than conventional CT doses.[19,20]

The first CBCT, NewTom 9000 (Quantitative Radiology, Verona, Italy), was described in 1998.[21] Since then, several other CBCT systems have been

*Correspondence to: Maria Alves Garcia Silva, Rua 13, N0 778 – Setor Marista, 74150–140 Goiania, Goias, Brazil; E-mail: magss@odonto.ufg.br
Received 21 April 2007; revised 3 September 2007; accepted 9 September 2007

developed: Ortho-CT (Hitachi and Morita Co, Kyoto Japan),[1] 3DX MultiImage Micro-CT – 3D Accuitomo (Morita Co, Kyoto, Japan), DentoCAT™ (Xoran Technologies, Ann Arbor, MI), PSR9000N (Asahi Roentgen, Kyoto, Japan),[22] CBMercuRay (Hitachi Medical Systems America, Twinsburg, OH), i-CAT (Imaging Sciences International, Hatfield, PA) and ProMax 3D (Planmeca, Helsinki, Finland). Most recently, another machine (Veraviewepocs 3D, Morita, Kyoto, Japan) has become available.

The dosimetry relating to these pieces of equipment has been established[16–18,20,23–25] to provide the necessary information in relation to their risks and benefits. However, the dosimetry parameters have not yet been established for the new CBCT equipment. The aim of this study was to compare the effective dose from the new cone beam CT (Veraviewepocs 3D) to the 3D Accuitomo in different fields of view (FOVs).

Materials and methods

Dosimetry

Dose measurements were carried out on an anthropomorphic phantom especially designed for dosimetry studies in dental radiography. This phantom was developed and built at the University of Göttingen, Germany,[26]and consisted of 48 transverse sections, each 6 mm thick with small holes positioned perpendicular to the axial axis of the phantom (Figure 1). The dosimetric phantom is representative of the essential anatomical structures of the head and neck, including the eyes, salivary glands, thyroid, calcified tissues, nasopharyngeal canal, paranasal sinuses and the oesophagus. Lithium fluoride thermoluminescent dosemeter (TLD) chips (LiF:Mg,Cu,P), Harshaw TLD-100H (Thermo Electron Co, Oakwood Village, OH) were used. One of the advantages of LiF-based thermoluminescent materials is their tissue-equivalent properties. The absorbed doses at selected locations, corresponding to the radiosensitive organs of interest, were measured using a set of 48 TLDs. The 16 phantom sites both inside and on the surface of the phantom can be seen in Table 1. Three dosemeters were placed in each anatomical site to calculate the mean value of each location, while retaining the same dosemeters in the same positions for each exposure. Before the study, all dosemeters were calibrated using the same type and range of radiation that would be used during the experiments. Prior to every exposure, the dosemeters were annealed at 240℃ for 10 min and then cooled to 35℃. All TLDs were read immediately after each exposure using a Harshaw 5500 Series Automatic TLD Reader (Harshaw/Bicron, Solon, OH).

Exposures

The CBCT units used for this study were 3D Accuitomo (Morita, Kyoto, Japan) and Veraviewepocs 3D (Morita, Kyoto, Japan). Table 2 shows the technical parameters and FOV for each unit used. Taking the small amount of radiation and the exposure latitude of the TLDs into account, after loading with TLDs, the phantom was exposed five times in order to provide a reliable measurement of radiation by the dosemeters. Later, these values were divided by five to provide one individual value for each region. To compare the data, we used narrow and large FOVs for the anterior region of the maxilla for both Accuitomo and Veraviewepocs 3D. The X-ray parameters used were those appropriate for a young adult male. Since the phantom is composed of multiple slabs, various tapes were used for alignment and maintenance of their positions during the irradiation process. The phantom was positioned in accordance with

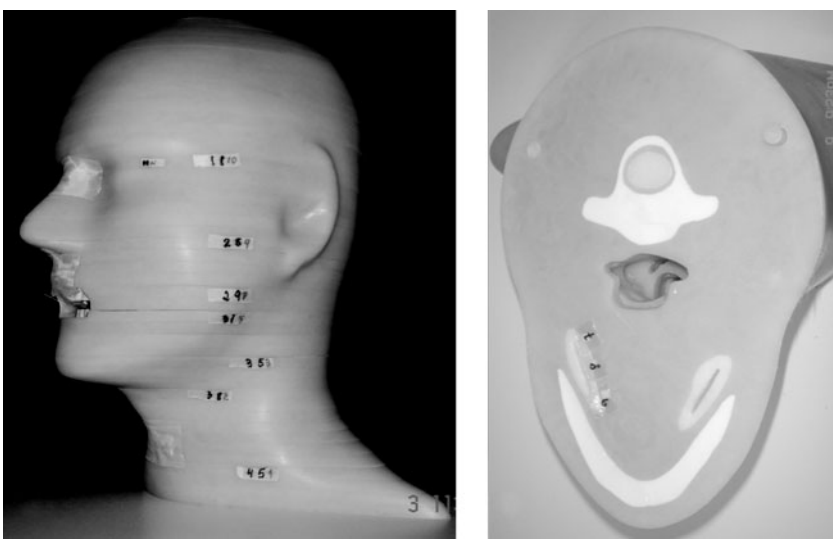

a b

Figure 1 (a) Adult skull and tissue equivalent phantom. Correspondent levels to thermoluminescent dosemeter (TLD) sites listed in Table 1. (b) TLDs packed before being positioned in the submandibular gland site

Table 1 Sites in which thermoluminescent dosemeter (TLD) 100H chips were placed

Organ related	*TLD location*	*Phantom level*
Bone marrow	Third cervical vertebra	45
	Mandibular ramus	31
Spine	Cervical	38
Brain	Hypophysis	18
Eye	Lens	18
	Upper and lower premolar	29, 31
	Maxillary sinus floor	25
Thyroid	Thyroid gland	45
Salivary glands	Submandibular gland	35
	Parotid gland	29
Skin	Thyroid	43
	Neck (back)	34
	Philtrum	27
	Parotid	27
	Nasion	18

Table 2 Technical parameters and field of view (FOV) exposure of the phantom

	FOV	*Tube energy (kV)*	*Tube current (mA)*
Veraviewepocs 3D	8 × 4 cm	80	4
Veraviewepocs 3D	4 × 4 cm	80	4
Veraviewepocs 3D	Panoramic view	70	5
	+ anterior 4 × 4	80	4
3D Accuitomo	6 × 6 cm	80	4
3D Accuitomo	4 × 4 cm	80	4

the manufacturer's specifications for each machine, following the reference lines and head rests. The standard examination was carried out for each unit and the dosimetry was performed three times for each technique in order to ensure reliability.

Dose calculations

After reading, an individual sensitivity value was applied for each TLD. Exposure doses were recorded in nanocoulombs (nC) and, after the application of energy calibration factors (RCF, reader calibration factor; and ECC, element correction coefficient), the dosimetry data were converted into milligrays (mGy) and subsequently recorded. The standard deviation of the readings from TLD-100H is less than ±5%. Doses from the three TLDs located in the same tissue or organ were averaged, resulting in the organ dose. The weighted dose for bone marrow was calculated using the sum of the radiation from the third cervical vertebra and the mandibular ramus. Both the submandibular and parotid salivary gland doses were used for calculating the weighted dose for salivary glands. The thyroid gland dose was individually calculated taking its specific weighted factor into consideration. For the skin surface area, five points were measured: thyroid skin, neck (back), philtrum, parotid and nasium skin. These same measurements were used to calculate the equivalent dose (H_T) according to the equation: $H_T = \sum W_R \times D_T$, where the equivalent dose (H_T) for a tissue or organ is the product of the radiation weighting factor (W_R) and the average absorbed dose (D_T) measured for that specific organ.[27] The equivalent dose is used to compare the effects of different types of radiation on tissues or organs, presented as *s*ievert (Sv).

The effective dose (E) is a calculation proposed by the International Commission on Radiological Protection (ICRP).[27] This dose is calculated by multiplying actual organ doses by "risk weighting factors" (associated with individual organ sensitivities) and represents the dose that the total body could receive and that would provide the same cancer risk as the application of different doses to various organs (an effective human equivalent dose or effective dose).[27] This effective dose was calculated as follows: $E = \sum W_T \times H_T$, where E is the product of the ICRPs tissue weighting factor (W_T) for the type of tissue or body and the human-equivalent dose for tissue (H_T). The tissue weighting factor represents the contribution that each specific tissue or organ makes to the overall risk. This dose was expressed in microsieverts. In this study we used the weighting factors, including salivary tissue in the risk estimation, as proposed by the ICRP in 2005[28] and approved by the ICRP Main Commission at its March 2007 Meeting.

Results

The averaged organ absorbed doses are presented in Table 3. The mean value was obtained from nine

Table 3 Mean absorbed dose (μGy) in various tissues for each unit and field of view

		Veraview 3D (8 × 4 – ant)	*Veraview 3D (4 × 4 – ant)*	*Veraview 3D (pan + 1 scan 4 × 4)*	*Accuitomo (6 × 6 – ant)*	*Accuitomo (4 × 4 – ant)*
Bone marrow	Third cervical vertebra	400.9	251.7	102.8	314.8	94.1
	Mandibular ramus	1321.3	1196.7	1211.9	1472.0	824.6
Brain	Hypophysis	108.4	35.7	54.8	108.0	31.6
Eye	Lens	275.5	54.7	75.1	104.6	31.6
Thyroid	Thyroid gland	87.3	56.2	39.0	115.6	42.8
Salivary glands	Submandibular gland	428.4	275.8	185.6	958.6	250.4
	Parotid gland	2490.3	2022.8	2258.5	2242.0	1268.8
Skin	Thyroid	53.6	34.4	25.2	66.9	25.2
	Neck (back)	2201.7	1276.5	333.6	353.8	108.9
	Philtrum	4095.6	3395.0	3200.0	10328.4	2803.2
	Parotid	3689.9	438.5	2687.4	2817.5	450.0
	Nasion	321.9	65.4	94.2	124.9	36.1

ant, anterior; pan, panoramic

measures for each technique and site (three dosemeters in each site, performed three times). The lowest organ dose was received by the thyroid skin during the Veraviewepocs 3D (Panoramic + anterior scan 4×4) and 3D Accuitomo (4×4) examinations. The highest organ dose was associated with the philtrum skin for the Veraviewepocs 3D (panoramic + anterior scan 4×4). Table 4 displays equivalent dose calculations, expressed in microsieverts. It can be seen that the lowest value was for Veraviewepocs 3D during the panoramic examination associated with a single anterior 4×4 cm scan. Doses reported in the literature concerning other CBCT units are shown in Table 5. For comparison, the data were converted to microsieverts.

Discussion

The selection criteria must always follow the ALARA (As Low As Reasonably Achievable) principle,[27] no matter what image is taken of a patient. Since their introduction in 1998, CBCT equipment has been undergoing evaluation so as to offer better images and more suitable machinery. Some machines have larger FOVs which provide information on the whole head, or at least on both the maxilla and mandible, varying from 13 cm (i-CAT) to 30 cm FOVs (CBMercuRay, i-CAT and NewTom). However, images of just teeth and alveolar bone are often necessary for dental practice. In these cases, narrow FOVs of 3×4 cm, 4×4 cm or 6×6 cm, respectively, are available and most recently a 4×8 cm FOV has become available. But how this small difference in size could affect the patient dosage was as yet unknown.

The Veraviewepocs 3D is a dental panoramic X-ray unit with a high-frequency switching mode X-ray generator. In addition to providing panoramic exposure, the unit can also take scanograms. A CBCT unit is also available that uses a cone shaped X-ray beam projected onto a flat panel detector. Its operating tube potential varies from 60 kV to 90 kV (± 1 kV, 21 steps) and its operating tube current ranges from 1 mA to 10 mA. The pixel size of the sensor is 0.048 mm for digital panoramic and 0.174 mm for CT and resolution of more than 2 lp mm^{-1}.

In this study, the dose associated with the Veraviewepocs 3D 4×4 cm (30.2 μSv) was higher than that from the Accuitomo 4×4 cm (20.0 μSv). Since the same technical parameters were used for both machines (Table 2), this difference can be explained by the smaller source to object distance in Veraviewepocs 3D (34.5 cm) than in the 3D Accuitomo (40 cm). However, the dose associated with the panoramic view + sectional 4×4 was even lower (29.7 μSv) than that related to the sectional view alone (30.2 μSv). The shorter time required for the panoramic scanning (7.4 s) probably leads to a lesser exposure than the two scouts required for the sectional image itself. According to our results, we recommend that the choice of region for scanning be based on a previous panoramic view, due to the following advantages: (1) the clinician has a general view of the maxilla and mandible; (2) it is easier to choose the region for scanning from a panoramic view than from a ''scout''; and (3) this results in a lower exposure dosage to the patient than when the scan is used in isolation.

On comparing both machines (Veraviewepocs 3D and 3D Accuitomo), it can be seen that the dose delivered from the narrow FOV was lower than that from the larger FOV. When taking both the image required and the clinical necessities into consideration, this dose can be justified. Although the FOVs did not differ greatly, the 3D Accuitomo 6×6 cm delivered a higher dose to the patient than the Veraviewepocs 3D 8×4 cm. Considering the larger scanning rotation of the 3D Accuitomo (360°) when compared with the Veraviewepocs 3D (just 180° around the patient's head), even less radiation should be expected from the latter. The doses obtained are difficult to compare with previous studies due to the many different experimental parameters: machines, protocols (different portions of the head and neck exposed), technical parameters (operational setting as kV and mA), methods of measurement and dosimetry systems. For this reason, we just compared the total effective dose (Table 4), considering that it is usually calculated in the same way and constitutes a good parameter. So, the effective doses for the 3D Accuitomo and the Veraviewepocs 3D are lower than the doses described for the NewTom 9000,[23,24] i-CAT 23 cm or 30.5 cm FOV[20] and much lower than the doses reported for conventional[17,19] or

Table 4 Mean equivalent dose (μSv) and effective dose (μSv) for each unit and field of view

	Veraview 3D (8×4 – ant)	*Veraview 3D (4×4 – ant)*	*Veraview 3D (Pan + 1 scan 4×4)*	*Accuitomo (6×6 – ant)*	*Accuitomo (4×4 – ant)*
Bone marrow*	861.10	724.20	657.35	893.40	414.35
Brain	108.40	35.70	54.80	108.00	31.60
Eye	275.50	54.70	75.10	104.60	31.60
Thyroid gland	87.30	56.20	39.00	115.60	42.80
Salivary glands†	1459.35	1149.30	1222.05	100.30	759.60
Skin**	2072.54	1041.96	6340.40	2738.30	686.68
Effective dose	39.92	30.24	29.78	43.27	20.02

*Mean of mandibular ramus and cervical spine; †Mean of Submandibular and parotid glands; **Mean of thyroid skin, neck, philtrum, parotid, and nasium skin. ant, anterior; pan, panoramic

Table 5 Comparisons of doses with various cone beam CT (CBCT) units from the literature

Author	*CBCT unit*	*FOV (cm)*	*Total dose (μSv)*
Mozzo et al, 1998[21]	NewTom 9000	23	3000.0–9000.0
Cohnen et al, 2002[25]	NewTom 9000	23	110.0
Mah et al, 2003[24]	NewTom 9000	23	50.3
Ludlow et al, 2003*,[23]	NewTom 9000	23	77.9
Hashimoto et al 2003[129]	3DX MultiImage Micro-CT	2.8 × 3.8	1190.0
Tsilakis et al, 2005*,[16]	NewTom 9000	23	52.0
Ludlow et al, 2006**,[20]	NewTom 3G	30.5	58.9
	CBMercuRay	30.5	1025.4
		23	435.5
		15	283.3
	i-CAT	30.5	193.4
		23	104.5

*Including salivary glands; †only skin dose measurements; **considering W_T from 2005 ICRP; FOV, field of view

multislice CT.[30–32] Even considering that the dose related to dentomaxillofacial radiology is very low, the extent of the risk remains uncertain, especially for critical organs such as the salivary and thyroid glands.[33,34] However, the cancer risk induced by low-dose dental radiology has been well established.[35] Advanced imaging procedures are usually associated with a higher dose to the patient, especially when tomographic X-ray images are used. The new cone beam technology provides high quality image information and delivers very low patient doses.

This study set out to compare the effective dose from both pieces of equipment, the Veraviewepocs 3D and 3D Accuitomo. A subjective evaluation of imaging performance proved that CBCT was better than the four-row multidetector helical CT.[36] Holbeg et al[37] found better visualization for the periodontal ligament space using CT compared with CBCT, although no statistical tests were applied to their results. Swennen and Schutyser[38] highlighted the limitations of CBCT for orthodontic purposes, such as the scanning volume and restricted FOV, when compared with multislice CT. Nevertheless, there are no comparisons of different types of cone beam CT relating to the image quality. Objective studies are necessary to investigate the image quality and its impact on the diagnostic performance of different CBCT units, and thus decision making balances between patient benefit and the risks associated with the X-ray exposure.

In the near future, machines with a greater variety of FOVs (both narrower and larger) will probably become available, making it possible to choose the appropriate FOV for a particular clinical question. Therefore, the ideal machine should allow for the choice between an exclusively dental and alveolar bone image (4 cm or 6 cm FOV) and a wider view (20 cm or 30 cm) necessary for traumatology and orthodontic procedures. This study evaluated the effective dose within specific technical parameters and for one specific region where many TLDs were positioned. If a different region had been considered, a lower radiation dosage may have been obtained. Possibly more important than choosing the best equipment is decision making in clinical practices, where clinicians need to be conscious of the kind of image that is really necessary. Healthcare professionals should be adequately trained and aware of the need to use the lowest tube energy and tube current possible, balanced with image quality. For many years, the prescribing of imaging has been the main topic in radiation protection.[39] Although the doses are very low, it is our responsibility to ensure that the patient does not receive unnecessary radiation. It is therefore important to highlight the fact that a cone beam still delivers more radiation than panoramic or individual periapical images.[20,40–42] Hence CBCT is indicated in clinical situations where there is a clear necessity for 3D analysis.

In conclusion, the radiation dose delivered from both machines falls into comparable ranges when using 4 × 4 cm FOV. A smaller FOV should be used for dental images and the larger FOV should be restricted to cases in which a wider view is required. The choice should be based on the clinical issues and ALARA principles.

Acknowledgments

This study was supported by CAPES – Brazilian Foundation.

References

1. Arai Y, Tammisalo E, Hashimoto K, Shinoda K. Development of a computed tomographic apparatus for dental use. *Dentomaxillofac Radiol* 1999; **28**: 245–248.
2. Sukovic P. Cone beam computed tomography in craniofacial imaging. *Orthod Craniofacial Res* 2003; **6(Suppl. 1)**: 31–36.
3. Guerrero ME, Jacobs R, Loubele M, Schutyser F, Suetens P, van Steenberghe D. State-of-the-art on cone beam CT imaging for preoperative planning of implant placement. *Clin Oral Invest* 2006; **10**: 1–7.
4. Aranyarachkul P, Caruso J, Gantes B, Schulz E, Riggs M, Dus I, et al. Bone density assessment of dental implant sites: 2. Quantitative cone-beam computerized tomography. *Int J Oral Maxillofac Implants* 2005; **20**: 416–424.
5. Hamada Y, Kondoh T, Noguchi K, Lino M, Isono H, Ishi H, et al. Application of limited cone beam computed tomography to clinical assessment of alveolar bone grafting: a preliminary report. *Cleft Palate Craniofac J* 2005; **42**: 128–137.

6. Cevidanes LHS, Bailey LJ, Tucker GR, Styner MA, Mol A, Phillips CL, et al. Superimposition of 3D cone-beam CT models of orthognathic surgery patients. *Dentomaxillofac Radiol* 2005; **34**: 369–735.
7. Lofthag-Hansen S, Huumonen S, Gröndahl K, Gröndahl H-G. Limited cone-beam CT and intraoral radiography for the diagnosis of periapical pathology. *Oral Surg Oral Med Oral Pathol Oral Radiol Endod* 2007; **103**: 114–119.
8. Stavropoulos A, Wenzel A. Accuracy of cone beam dental CT, intraoral digital and conventional film radiography for the detection of periapical lesions. An ex vivo study in pig jaws. *Clin Oral Investig* 2007; **1**: 101–106.
9. Misch KA, Yi RS, Sarment DP. Accuracy of cone beam computed tomography for periodontal defect measurements. *J Periodontol* 2006; **77**: 1261–1266.
10. Honda K, Arai Y, Takano Y, Sawada K, Ejima K, Iwai K. Evaluation of the usefulness of the limited cone-beam CT (3DX) in the assessment of the thickness of the roof of the glenoid fossa of the temporomandibular joint. *Dentomaxillofac Radiol* 2004; **33**: 391–395.
11. Honda K, Larheim TA, Matsumoto K, Iwai K. Osseous abnormalities of the mandibular condyle: diagnostic reliability of cone beam computed tomography compared with helical computed tomography based on an autopsy material. *Dentomaxillofac Radiol* 2006; **35**: 152–157.
12. Nakajima A, Sameshima GT, Arai Y, Homme Y, Shimizu N, Dougherty H. Two- and three-dimensional orthodontic imaging using limited cone beam-computed tomography. *Angle Orthod* 2005; **75**: 895–903.
13. Swennen GRJ, Schtyser F. Three-dimensional cephalometry: spiral multi-slice vs cone-beam computed tomography. *Am J Orthod Dentofacial Orthop* 2006; **130**: 410–416.
14. Yang F, Jacobs R, Willems G. Dental age estimation through volume matching of teeth imaged by cone-beam CT. *Forensic Sci Int* 2006; **159(Suppl. 1)**: S78–S83.
15. Farman AG, Scarfe WC. Development of imaging selection criteria and procedures should precede cephalometric assessment with cone-beam computed tomography. *Am J Orthod Dentofacial Orthop* 2006; **130**: 257–265.
16. Tsilakis K, Donta C, Gavala S, Karayianni K, Kamenopoulou V, Hourdakis CJ. Dose reduction in maxillofacial imaging using low dose cone beam CT. *Eur J Radiol* 2005; **56**: 413–417.
17. Lecomber AR, Yoneyama Y, Lovelock DJ, Hosoi T, Adams AM. Comparison of patient dose from imaging protocols for dental implant planning using conventional radiography and computed tomography. *Dentomaxillofac Radiol* 2001; **30**: 255–259.
18. Schulze D, Heiland M, Thurman H, Adam G. Radiation exposure during midfacial imaging using 4- and 16-slice computed tomography, cone beam computed tomography systems and conventional radiography. *Dentomaxillofacial Radiol* 2004; **33**: 83–86.
19. Frederiksen NL, Benson BW, Sokolowski TW. Effective dose and risk assessment from film tomography used for dental implant diagnostics. *Dentomaxillofac Radiol* 1994; **23**: 123–127.
20. Ludlow JB, Davies-Ludlow LE, Brooks SL, Howerton WB. Dosimetry of 3 CBCT devices for oral and maxillofacial radiology: CB Mercuray, NewTom 3G and i-CAT. *Dentomaxillofac Radiol* 2006; **35**: 219–226.
21. Mozzo P, Procacci C, Tacconi A, Tinazzi Martini P, Bergamo Andreis IA. A new volumetric machine for dental imaging based on the cone-beam technique: preliminary results. *Eur Radiol* 1998; **8**: 1558–1564.
22. Yammamoto K, Ueno K, Seo K, Shinohara D. Development of dento-maxillofacial cone beam X-ray computed tomography system. *Orthod Craniofacial Res* 2003; **6(Suppl. 1)**: 160–162.
23. Ludlow JB, Davies-Ludlow LE, Brooks SL. Dosimetry of two direct digital imaging devices: NewTom cone beam CT and Orthophos Plus DS panoramic unit. *Dentomaxillofac Radiol* 2003; **32**: 229–234.
24. Mah JK, Danforth RA, Bumann A, Hatcher D. Radiation absorbed in maxillofacial imaging with a new dental computed tomography device. *Oral Surg Oral Med Oral Pathol Oral Radiol Endod* 2003; **96**: 508–13.
25. Cohnen M, Kemper J, Mobes O, Pawelzik J, Modder U. Radiation dose in dental radiology. *Eur Radiol* 2002; **12**: 634–637.
26. Visser H. *Investigations into the optimization of periodontal radiography* (Untersuchungen zur optimierung der parodontologischen Röntgen diagnostik). Berlin, Germany: Quintessenz Publishing, 2000.
27. International Commission on Radiation Protection. 1990 Recommendations of the International Commission on Radiological Protection, ICRP Publication 60. *Ann ICRP* 1991; **21**: 1–201.
28. Recommendations of the International Commission on Radiological Protection. ICRP htpp://www.icrp.org [Accessed 05 April 2007].
29. Hashimoto K, Yoshinori A, Iwai K, Araki M, Kawashima S, Terakado M, et al. A comparison of new limited cone beam computed tomography machine for dental use with a multidetector row helical CT machine. *Oral Surg Oral Med Oral Pathol Oral Radiol Endod* 2003; **95**: 371–7.
30. Frederiksen NL, Benson BW, Sokolowski TW. Effective dose and risk assessment from computed tomography of the maxillofacial complex. *Dentomaxillofac Radiol* 1994; **24**: 55–58.
31. Dula K, Mini R, van der Stelt PF, Sanderink GCH, Schneeberger P, Buser D. Comparative dose measurements by spiral tomography for preimplant diagnosis: the Scanora machine versus the Cranex Tome radiography unit. *Oral Surg Oral Med Oral Pathol Oral Radiol Endod* 2001; **91**: 735–742.
32. Dula K, Mini R, van der Stelt PF, Lambrecht JT, Schneeberger P, Buser D. Hypothetical mortality risk associated with spiral computed tomography of the maxilla and mandible. *Eur J Oral Sci* 1996; **104**: 503–510.
33. Underhill TE, Chilvarquer I, Kimura K, Langlais RP, McDavid WD, Preece JW, et al. Radiobiologic risk estimation from dental radiology. Part I. Absorbed doses to critical organs. *Oral Surg Oral Med Oral Pathol* 1988; **66**: 111–120.
34. Underhill TE, Kimura K, Chilvarquer I, McDavid WD, Langlais RP, Preece JW, et al. Radiobiologic risk estimation from dental radiology. Part II. Cancer incidence and fatality. *Oral Surg Oral Med Oral Pathol* 1988; **66**: 161–167.
35. Ron E. Cancer risks from medical radiation. *Health Phys* 2003; **1**: 47–59.
36. Hashimoto K, Kawashima S, Araki M, Iwai K, Sawada K, Akiyama Y. Comparison of image performance between cone-beam computed tomography for dental use and four-row multidetector helical CT. *J Oral Science* 2006; **48**: 27–34.
37. Holberg C, Steinhäuser S, Geis P, Rudzki-Janson I. Cone beam computed tomography in orthodontics: benefits and limitations. *J Orofac Orthop* 2005; **66**: 434–444.
38. Swennen GRJ, Schtyser F. Three-dimensional cephalometry: spiral multi-slice vs cone-beam computed tomography. *Am J Orthod Dentofacial Orthop* 2006; **130**: 410–416.
39. Tyndall DA, Brooks SL. Selection criteria for dental implant site imaging: a position paper of the American Academy of Oral and Maxillofacial Radiology. *Oral Surg Oral Med Oral Pathol Oral Radiol Endod* 2000; **89**: 630–637.
40. Danforth RA, Clark DE. Effective dose from radiation absorbed during a panoramic examination with a new generation machine. *Oral Surg Oral Med Oral Pathol Oral Radiol Endod* 2000; **89**: 236–243.
41. Clark DE, Danforth RA, Barnes RW, Burtch ML. Radiation absorbed dose from dental implant radiography: a comparison of linear tomography, CT scan, and panoramic and intra-oral techniques. *J Oral Implantol* 1990; **3**: 156–164.
42. Gibbs SJ. Effective dose equivalent and effective dose: comparison for common projections in oral and maxillofacial radiology. *Oral Surg Oral Med Oral Pathol Oral Radiol Endod* 2000; **90**: 538–545.